scientific reports

Check for updates

OPEN

Radiosensitizing effects of Withaferin A in gastric cancer cells via autophagy Inhibition and mitochondrial disruption

Ping Lu[1]✉, Juan Xue[2] & Xuemeng JI[3]✉

Gastric cancer is highly lethal due to late-stage diagnosis and resistance to standard treatments like radiotherapy. Enhancing radiosensitivity in gastric cancer cells could improve treatment outcomes. Withaferin A (WA), a bioactive compound from *Withania somnifera*, has anticancer effects and can modulate cellular processes like autophagy and mitochondrial function. This study investigates WA's role in enhancing radiosensitivity by targeting apoptosis, autophagy, and mitochondrial function in SGC-7901 gastric cancer cells. In both in vitro and in vivo models, combined WA and radiation (IR) treatment significantly inhibited tumor growth, as evidenced by reduced tumor size in xenografts. Mechanistically, this combination promoted apoptosis, with increased levels of cleaved caspase-3 and PARP, indicating enhanced cell death. WA altered autophagic dynamics by activating autophagy and blocking autophagic flux, shown by LC3II accumulation and SQSTM1/p62 buildup. Moreover, the combined treatment disrupted mitochondrial function, leading to decreased ATP production, reduced respiratory capacity, and increased proton leakage, which contributed to cellular stress. These findings suggest that WA may serve as a radiosensitizer to enhance radiotherapy efficacy in gastric cancer, highlighting its therapeutic potential and advocating for further exploration of phytocompounds in cancer treatment.

Keywords Withaferin A, Autophagy, Radiotherapy, Gastric cancer, Radiosensitizer

Gastric cancer is one of the most prevalent and deadly cancers worldwide, with high mortality rates attributed to late-stage diagnosis, limited treatment options, and resistance to conventional therapies[1]. Standard treatments for gastric cancer, including chemotherapy, radiation therapy, and surgery, often yield suboptimal outcomes, particularly for patients with advanced or metastatic disease[2]. Radiation therapy (RT) remains an essential treatment modality; however, the inherent resistance of gastric cancer cells to radiation limits its effectiveness[3]. Thus, identifying agents that can enhance the radiosensitivity of gastric cancer cells presents a promising strategy to improve therapeutic outcomes.

Withaferin A (WA) is the most active phytocompound extracted from the renowned dietary supplement *Withania somnifera*, commonly known as Ashwagandha[4]and has shown potential as an anticancer agent in various malignancies, including breast[5] prostate[6] and pancreatic cancers[7]. WA has been reported to induce apoptosis, suppress metastasis, and inhibit angiogenesis, largely by affecting signaling pathways critical for cell survival and stress response[8,9]. Recent studies have highlighted WA's potential to disrupt cellular homeostasis by modulating processes like autophagy[7,10,11] and mitochondrial function[12,13]. However, the potential of WA to enhance radiosensitivity, specifically in gastric cancer cells, has not been fully explored. Understanding how WA may interact with radiation therapy to enhance its effects could reveal new avenues for combination therapies targeting gastric cancer.

Autophagy, a critical cellular process for maintaining homeostasis under stress, is often dysregulated in cancer[14,15]. Autophagy enables cancer cells to adapt to stress conditions, including nutrient deprivation and hypoxia, by degrading and recycling intracellular components[16]. While autophagy can be tumor-suppressive in early cancer stages, in established tumors, it may contribute to therapy resistance by enabling cancer cells to survive under adverse conditions[17,18]. The modulation of autophagy in response to radiation, particularly

[1]Tianjin Eye Institute, Tianjin Key Laboratory of Ophthalmology and Visual Science, Tianjin Eye Hospital, Nankai University Affiliated Eye Hospital, Nankai University Eye Institute, Tianjin 300020, China. [2]Institute of Infection and Immunity, Taihe Hospital, Hubei University of Medicine, Shiyan 442099, Hubei, China. [3]School of Medicine, Nankai University, Tianjin 300071, China. ✉email: luping-ykyjs@outlook.com; jixuemeng@nankai.edu.cn

in combination with WA, may therefore represent a strategic approach to sensitize cancer cells to treatment. Additionally, targeting mitochondrial function is emerging as a promising strategy in cancer therapy, given mitochondria's crucial role in regulating cell survival, bioenergetics, and apoptosis[19–21].

This study investigates the effects of WA in combination with radiation on gastric cancer cells, with a focus on autophagy modulation and mitochondrial function. The hypothesis is that WA could enhance the radiosensitivity of gastric cancer cells by inducing apoptosis and impairing autophagic flux, thus disrupting cellular homeostasis. Using both in vitro and in vivo models, this research evaluates the impact of combined WA and radiation treatment on tumor growth, apoptosis, autophagy dynamics, and mitochondrial integrity. The findings aim to provide insight into the potential of WA as a radiosensitizer in gastric cancer, supporting the development of novel combination therapies for improved cancer treatment outcomes.

Methods

Cell culture and IR

The human GC cell line SGC-7901 was obtained from American Type Culture Collection (ATCC). SGC-7901 cells were cultured in Roswell Park Memorial Institute (RPMI-1640) medium (Thermo) containing 10% heat-inactivated foetal bovine serum and 1% penicillin/streptomycin (Solarbio, China). The cells were incubated at 37 °C in a humidified chamber with 5% CO_2. The cells were exposed to one of several dosages of ionizing radiation (IR) 2, 4, 6, 8, and 10 Gy) using an X-ray linear accelerator (Rad Source Technologies, USA) at a fixed dose rate of 1.15 Gy/min. HUVECs were purchased from the ATCC. Cells were cultured in RPMI-1640 medium with 20% fetal bovine serum, 60 μg/mL of endothelial cell growth supplement (BD Biosciences, San Jose, CA), 1% penicillin/streptomycin at 37 °C in a humid atmosphere with 5% CO_2. IEC-6 cells were purchased from the ATCC and routinely cultured in DMEM medium with 1% antibiotics and 5% FBS at 37 °C in a humid atmosphere with 5% CO_2. 100 mM 3-MA or 100nM Bafilomycin A1 (BafA) was added for 2 h before the cells were challenged with WA and IR.

Cell proliferation assay and apoptosis assay

The Cell Counting Kit-8 (CCK-8) was employed to determine cell viability. SGC-7901 cells were seeded into 96-well plates, cultured overnight, and then treated with 20 μM WA (or 0.1% DMSO as a control) with or without one of several dosages of radiation. Ten microlitres of CCK-8 solution was added to each well, and the cells were incubated for 1 h before detection. Apoptosis was evaluated using a FITC Annexin V Apoptosis Detection Kit (Sigma-Aldrich, USA). The cells were stained with annexin V/propidium iodide (PI) and then detected by flow cytometry. The flow cytometry data were analysed using FlowJo software.

Caspase-3 and cleaved PARP detection by ELISA

For the quantification of caspase-3 and cleaved PARP, commercially available ELISA kits (Thermo) specific to human caspase-3 and cleaved PARP were used according to the manufacturer's instructions. Briefly, 100 μL of each cell lysate was added to the ELISA plate wells coated with capture antibodies. After incubation, wells were washed with PBS containing 0.05% Tween-20 to remove unbound material. Detection antibodies specific to cleaved forms of caspase-3 and PARP were then added, followed by a secondary antibody conjugated to horseradish peroxidase (HRP). The substrate solution was added, and the enzymatic reaction was stopped using a sulfuric acid solution once color development was sufficient. Optical density (OD) was measured at 450 nm using a microplate reader. Caspase-3 and cleaved PARP levels were calculated relative to control samples, with results normalized to total protein input.

Western blotting and immunocytochemistry

Xenograft tumours and cells were lysed with lysis buffer, and the extracted proteins were quantified, separated by SDS-PAGE, and then transferred to PVDF membranes. After blocking, the membranes were incubated at 4 °C overnight with the following primary antibodies(1:1000): cleaved caspase-3 antibody (ab2302;Abcam, Cambridge, UK), caspase-3 antibody (ab32351;Abcam), cleaved PARP1 antibody (ab32561;Abcam); PARP1 antibody (ab32138;Abcam); LC3A/B antibody (4108 S, Cell Signaling Technology, MA, USA), SQSTM1/p62 antibody (8025,Cell Signaling Technology), β-actin (3700 S, Cell Signaling Technology) and then with HRP-conjugated secondary antibodies (1:5000; Cell Signaling Technology) at room temperature for 1 h, followed by washing with TBST. The immunoblots were visualized by chemiluminescence. LC3 is now widely used to monitor autophagy. One approach is to detect LC3 conversion (LC3I to LC3II) because the amount of LC3II is clearly correlated with the number of autophagosome. The cells were inoculated onto a glass-bottom confocal dish and cultured for 24 h. WA (or 0.1% DMSO as a control) was then added with or without IR. At different time points, the cells were fixed with 4% (w/v) paraformaldehyde and 0.1% Triton-X for 10 min. The cells were then blocked with 5% (w/v) BSA in PBS at room temperature for 1 h, incubated in the dark for 1 h with primary antibodies (1:100) : LAMP1(ab24170;Abcam) and then incubated with a secondary antibody in the dark for 1 h. Cells were treated with 1 μg/ml acridine orange AO (ab270791;Abcam) or 50 ng/ml LysoTracker Red (L7528; Thermo fisher) for 30 min ;10 μg/ml DQ-BSA (D12051;Thermo fisher) for 2 h. The cell nuclei were stained with DAPI, and images were acquired with a Leica SPE confocal microscope.

Transfection with plasmids

SGC-7901Cells were transfected with Atg7-specific siRNA (Shanghai GenePharma Corporation) or plasmids expressing EGFP-LC3, mCherry-EGFP-LC3. Cells were transfected with 100 μl OptiMEM medium (Gibco/BRL) containing 1% Lipofectamine2000 (Invitrogen) and 20 pmol siRNA or 1 μg plasmid DNA.

Bioenergetic analysis

Bioenergetic profiles were detected using a Seahorse Bioscience Extracellular Flux Analyser XFe24 (Agilent, USA). Cells were inoculated into XFe24 cell culture plates and incubated with 20 μM WA for 30 min with or without 10 Gy radiation. The 103015-100 Seahorse XF Cell Mito Stress Test Kit was used to detect mitochondrial oxidative stress. The wells were then sequentially injected with oligomycin (1.5 μM), FCCP (1 μM), and rotenone/antimycin A (0.5 μM). The basal OCR was calculated as the OCR before oligomycin injection minus the OCR after antimycin injection. The maximal OCR was calculated as the OCR after FCCP injection minus the OCR after antimycin injection. The reserve capacity was calculated as the OCR after FCCP injection minus the OCR before oligomycin injection. The ATP-linked OCR was calculated as the OCR before minus the OCR after oligomycin injection. The proton leak OCR was calculated as the OCR after oligomycin injection minus the OCR after antimycin injection, and the nonmitochondrial OCR was defined as the OCR after antimycin injection.

Nude mice studies

Six-week-old male BALB/c nude mice ($N = 20$, average weight 22 ± 2 g), purchased from Vital River (Beijing Vital River Laboratory Animal Technology Co., Ltd.), were injected subcutaneously with SGC7901 cells (1×10^6), with or without irradiation, into their left posterior flank region. After 7 days, the mice were randomized into 4 groups; each group of five mice, 2 groups were injected with PBS as a negative control, and the other 2 group were injected with WFA 2 mg/kg. Mice were treated every other day i.p. using a volume of 100 μl. The experimental group underwent abdominal X-ray exposure using a calibrated X-ray machine. Only the abdominal region was exposed to the X-rays, while the rest of the body was covered with lead shielding to minimize radiation exposure to other tissues. Two of the groups were irradiated with a single dose of 10 Gy X-ray irradiation by linear accelerators at a dose rate of 1.15 Gy/min on day 7. Two-dimensional measurements were taken with an electronic calliper, and the tumour volumes were calculated in mm^3 using the following formula: volume = $A \times B^2/2$, where A is the longest diameter and B is the shortest diameter. Tumour volumes (mean ± s.e.m.; mm^3) were assessed every 2 days after day 7. After three weeks, all mice were euthanized. Euthanasia was performed via an intraperitoneal injection of pentobarbital sodium at a dose of 150 mg/kg body weight to induce deep anesthesia, followed by cervical dislocation to confirm death. Tissues were removed and fixed in 10% formalin for haematoxylin and eosin (H&E) staining. This study is reported in accordance with the ARRIVE guidelines (Animal Research: Reporting of In vivo Experiments) to ensure high standards of methodological rigor, transparency, and ethical compliance. All procedures were approved by the Animal Care and Use Committee.

Histology and scoring

Xenograft tumours were fixed in 10% formalin and embedded in paraffin for sectioning. Slides were deparaffinized in xylene and rehydrated in a graded series of ethanol. Antigen retrieval was conducted by incubating the slides in 10 mM sodium citrate, pH 6.0, for 20 min at 95 °C followed by treatment with 0.3% H_2O_2 in methanol for 20 min. Sections were incubated with primary antibodies against Ki67 diluted 1:50 (AbCam), CD31 1:50 (AbCam), LC3 1:500 (AbCam), and cleaved caspase 3 1:200 (Cell Signalling), at 4 °C overnight. Slides were rinsed with PBS and incubated with secondary antibody according to the suppliers' instructions. Colour was developed using DAB and counterstained with haematoxylin to stain nuclei as described previously. Digital images of two fields at ×400 magnification were acquired from each section, using an Olympus BX50 light microscope (Olympus Corporation, Tokyo, Japan). The most representative field was selected for image analysis. Images of five high power fields were acquired. Digital images were prepared for analysis using the ImageJ 1.44 program to calculate positively stained areas from the total epithelial area.

Statistical analysis

Statistical significance was analysed using the GraphPad Prism programme (version 8.4). Student's *t*-test was used to compare the statistical differences between two groups, while the differences among multiple groups were analyzed using One-way ANOVA. The data are represented as the mean and standard deviation. A p value < 0.05 was considered to be statistically significant.

Results

WA Enhances Tumor Cell Radiosensitivity by Promoting Apoptosis In vitro.

To assess the tumor selectivity and potential cytotoxicity of WA combined with radiation, both gastric cancer cells (SGC-7901) and non-tumor cell lines—human umbilical vein endothelial cells (HUVEC) and rat intestinal epithelial cells (IEC-6)—were evaluated. These two normal cell types were selected to represent radiosensitive vascular endothelium and gastrointestinal mucosa, which are commonly affected during radiotherapy. Cells were treated with increasing concentrations of WA followed by 10 Gy IR. All cell types exhibited a dose-dependent reduction in viability (Fig. 1A-D); however, SGC-7901 cells displayed the lowest IC50 (20 μM), indicating that tumor cells were more susceptible to WA-induced cytotoxicity compared to normal cells. These results suggest that WA may exert a preferential effect on cancer cells under irradiation. Further apoptosis assays revealed increased levels of cleaved caspase-3 and PARP in WA + IR-treated SGC-7901 cells (Fig. 1E, F), supporting the role of enhanced apoptosis in the radiosensitizing mechanism.

Combination of WA and radiation modulates early and late-stage autophagy

Autophagy pathway activation following the combined treatment of WA and radiation was evaluated by measuring the expression of the autophagy marker protein LC3. LC3II expression was notably elevated in the combined treatment group compared to the radiation-only group at 1 and 3 h post-treatment; however, by 18 h, LC3II levels showed no significant difference between groups (Fig. 2A-B). Additionally, LC3II expression

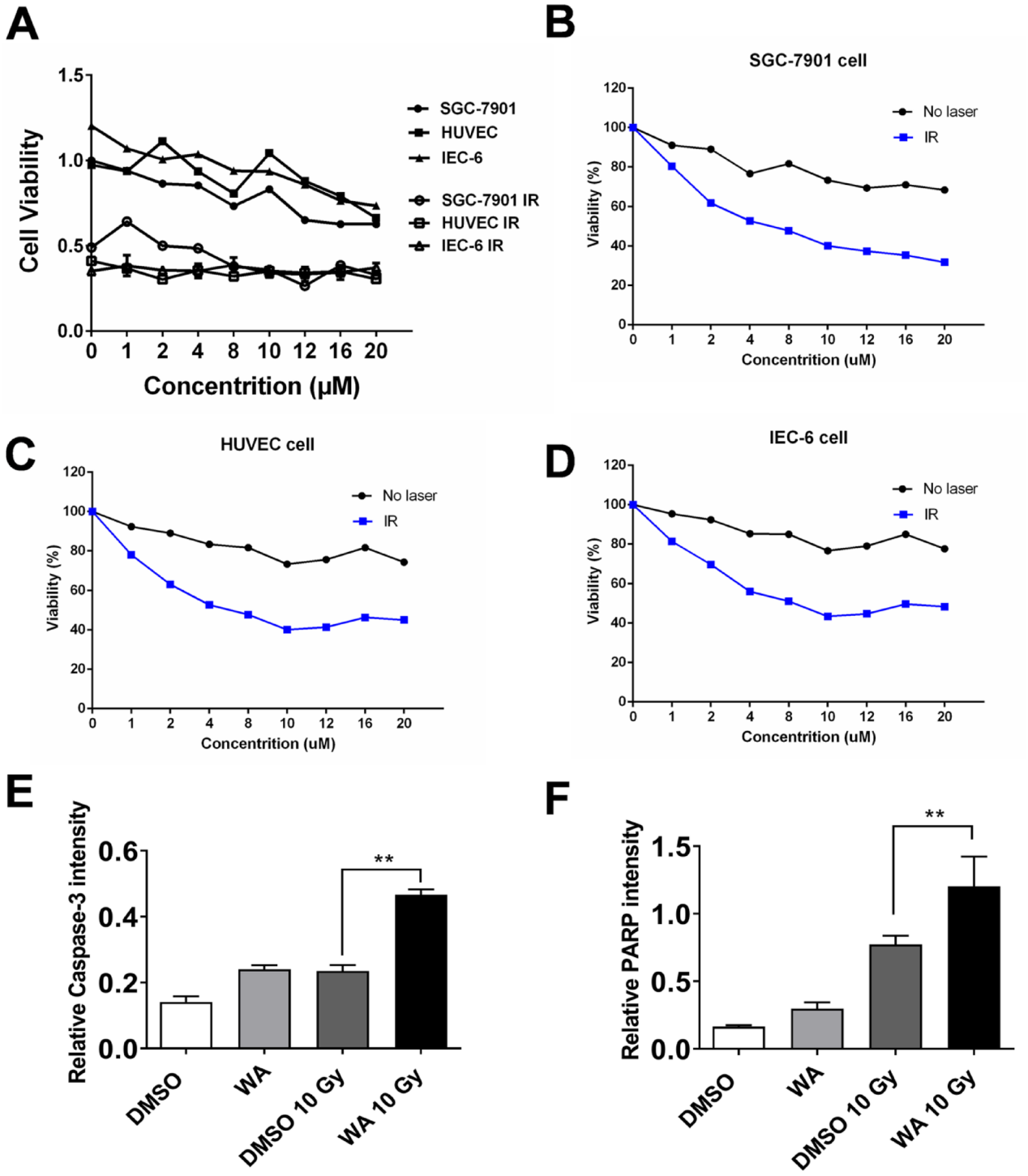

Fig. 1. Effects of WA and IR on cell viability and apoptosis. (**A**) Cell viability of SGC-7901, HUVEC, and IEC-6 cells treated with varying concentrations of WA (1, 2, 4, 8, 10, 12, 16, 20, 22, or 24 μM) for 30 min, followed by 10 Gy IR, assessed via CCK-8 assay. Viability values were normalized to the untreated control (0 μM WA, no IR). (**B**-**D**) Determination of half-maximal inhibitory concentration (IC50) of WA in SGC-7901, HUVEC and IEC-6 cells. Viability values were normalized to the IR-only group (0 μM WA + IR) and used to calculate IC50 values under irradiated conditions. (**E**) Expression of cleaved caspase-3 in SGC-7901 cells treated with 20 μM WA and 10 Gy IR at different time points (1, 3, 6, and 18 h). (**F**) Cleavage of poly ADP-ribose polymerase (PARP) in SGC-7901 cells following combined WA and IR treatment. Data are representative of three independent experiments.

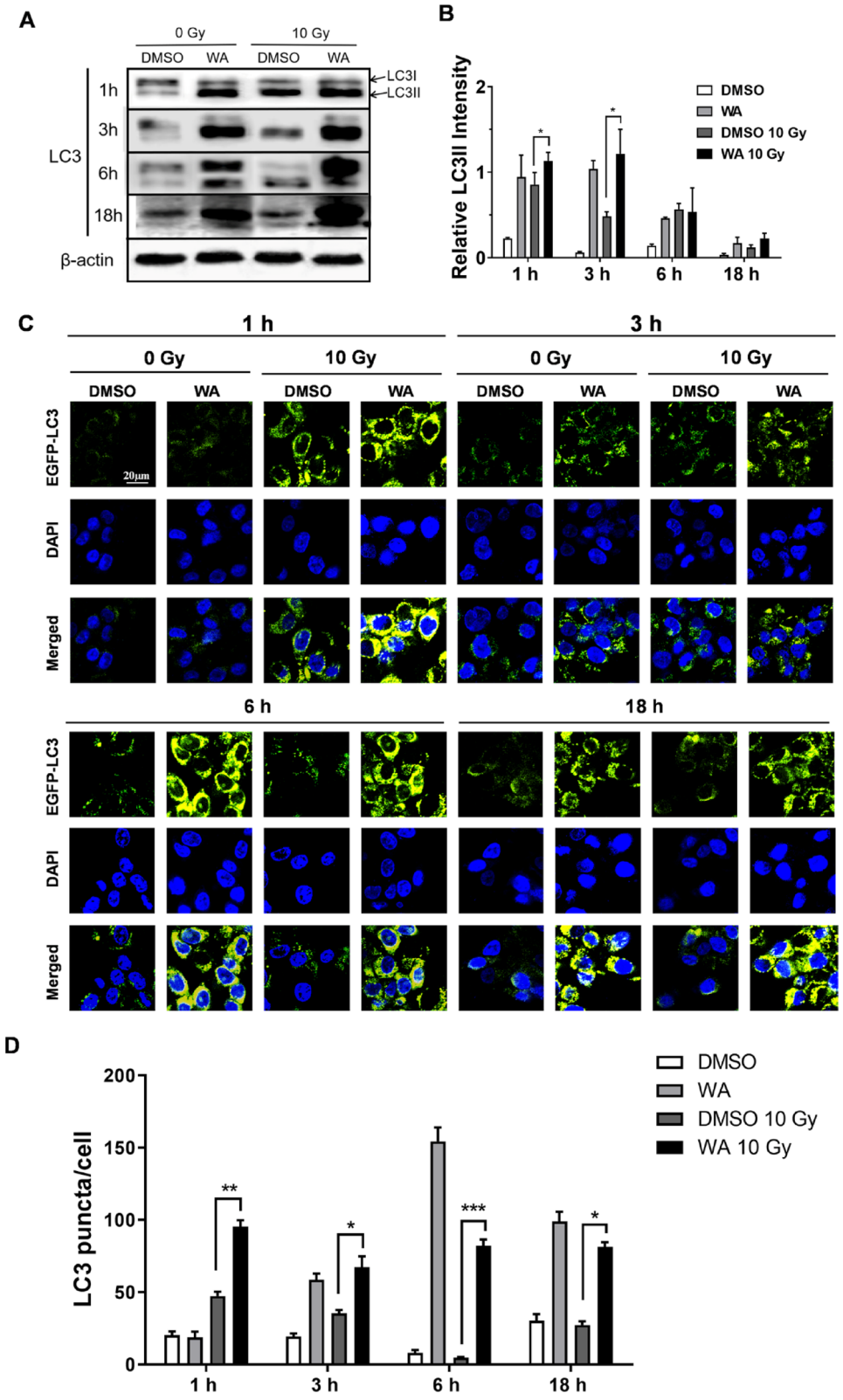

Fig. 2. The combination of WA and radiation induces autophagosome accumulation. (**A**-**B**) Western blot analysis of the autophagy marker protein LC3 in gastric cancer cells treated with 20 μM WA and 10 Gy radiation for 1 h, 3 h, 6 h, and 18 h (Raw blots are shown in Figure S1). Representative images from at least three independent biological replicates are presented. β-Actin was used as a loading control. (**C**-**D**) Confocal microscopy images showing EGFP-LC3 puncta (green), with cell nuclei stained using DAPI (blue). All images were acquired using identical confocal microscope settings (laser intensity, exposure time, and gain) across all groups to ensure comparability. All results are expressed as mean ± SD ($n = 3$). $^{*}P < 0.05$, $^{**}P < 0.01$, and $^{***}P < 0.001$.

levels in the WA-only and combined treatment groups remained similar at each time point (Fig. 2B). To further investigate autophagosome formation, cells were transfected with an EGFP-LC3 (green fluorescent protein-tagged LC3) reporter to visualize autophagic vacuoles. EGFP-LC3 distribution in the cytosol revealed autophagosome formation, as puncta were observed at 1, 3, and 6 h following IR exposure in the IR group, while the control group displayed diffuse green fluorescence (Fig. 2C-D). By 6 and 18 h, WA-treated cells showed a significantly higher number of LC3 puncta than the control group, regardless of IR exposure (Fig. 4D). EGFP-LC3 puncta visualization indicated that IR triggers early-stage autophagy activation, while WA appeared to modulate autophagy at later stages by inhibiting autophagic flux.

Combined WA and radiation treatment blocks autophagic flux

Autophagic flux was evaluated by analyzing the levels of the autophagic substrate SQSTM1/p62. Accumulation of p62 at 6 and 18 h in the combined treatment group suggested a blockage in autophagic flux beginning at 6 h (Fig. 3A-B). To further investigate autophagic flux, a dynamic assay was performed using SGC-7901 cells transfected with a fluorescent mCherry-EGFP-LC3 construct. In the combination treatment group, there was an increase in total puncta and red fluorescent puncta at 1, 3, and 6 h (Fig. 3C). By 6 and 18 h, however, the combined treatment showed a rise in yellow puncta and a decrease in red-only puncta, indicating impaired lysosomal function and reduced autophagosome degradation. These findings imply that WA and radiation together impair autophagosome clearance.

Combination of WA and radiation disrupts lysosomal degradation

To elucidate how the combination treatment hinders autophagosome degradation, three fundamental aspects of lysosomal function were evaluated. First, lysosomal membrane integrity was examined by quantifying levels of lysosome-associated membrane glycoprotein 1 (LAMP1). No significant changes were detected 18 h post-treatment (Fig. 4A-B), indicating that WA did not compromise lysosomal membrane integrity. Second,

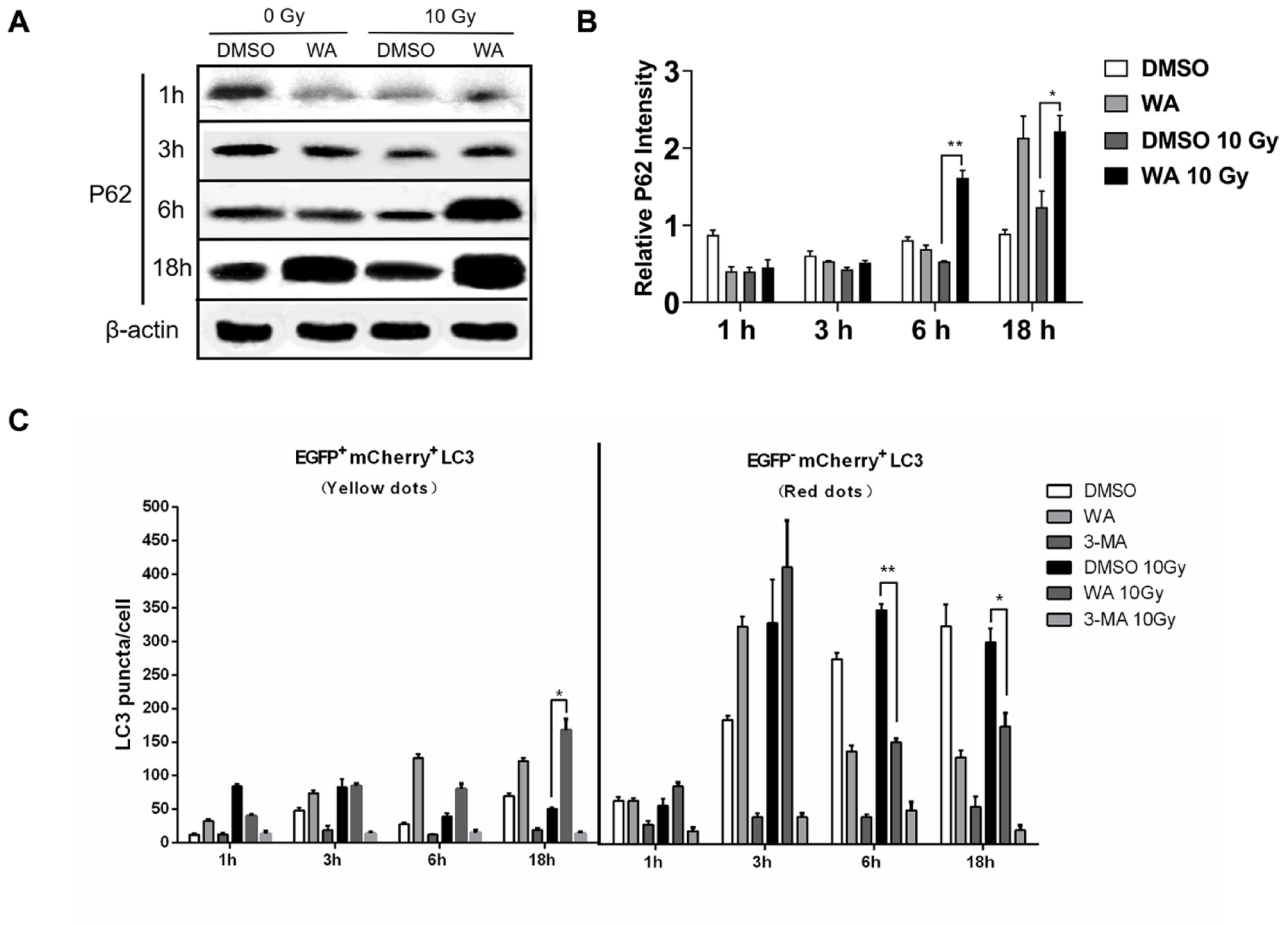

Fig. 3. WA inhibits lysosomal degradation. (**A**-**B**) Confocal microscopy analysis of SGC-7901 cells treated with WA (20 μM) for 30 min and 10 Gy radiation, followed by staining with phalloidin (green), LAMP1 (red), and DAPI (blue). (**C**-**D**) Cells were treated with both WA and radiation and then stained with acridine orange AO, (1 μg/ml) or LysoTracker Red (50 ng/ml) for 30 min. (**E**-**F**) SGC-7901 cells were stained with DQ-BSA (10 μg/ml) for 2 h and then treated with both WA and radiation. Representative fluorescence images are shown. Scale bars: 10 μm. All the results were shown as mean ± SD ($n = 3$). $^{*}P < 0.05$, $^{**}P < 0.01$ and $^{***}P < 0.001$.

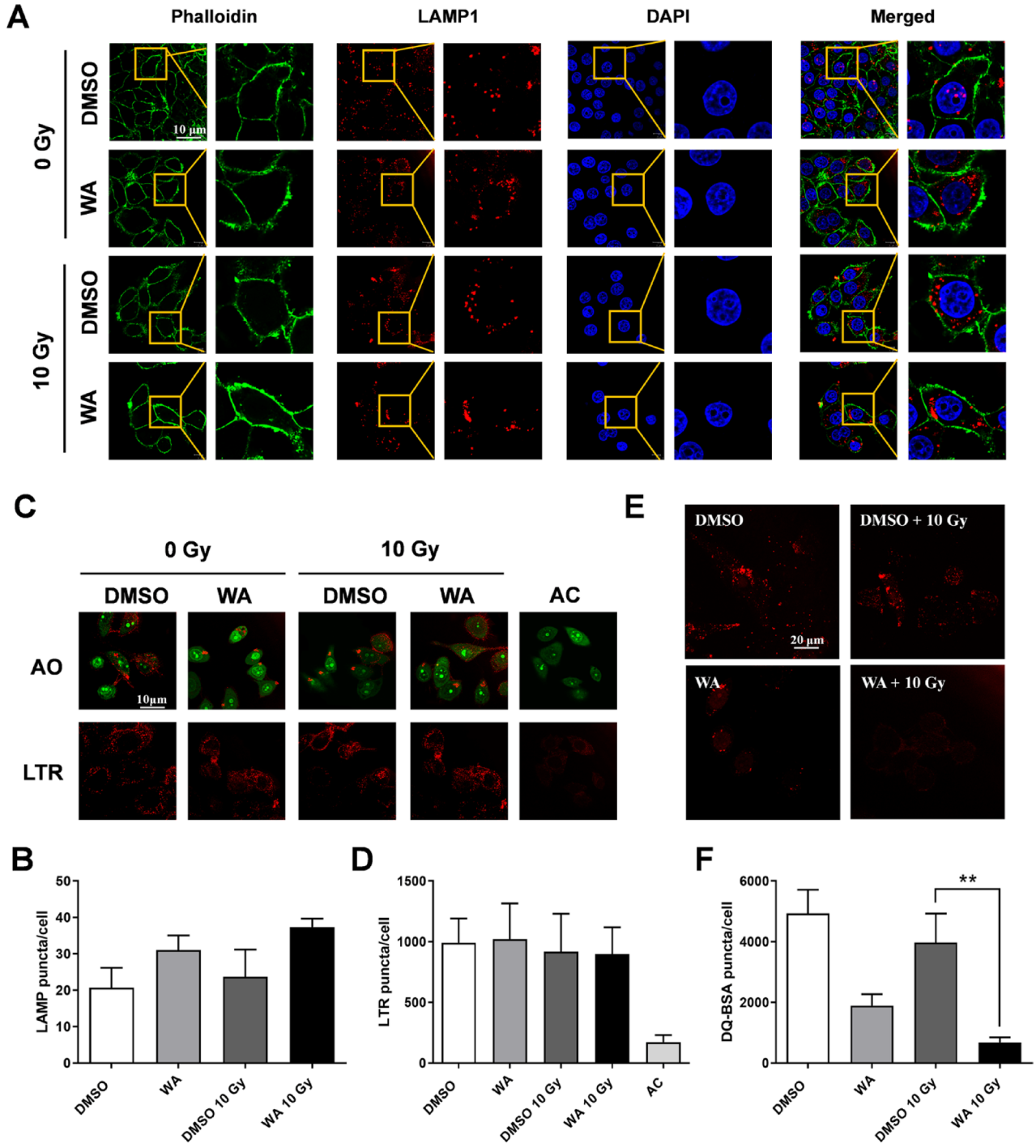

Fig. 4. WA inhibits autophagosome maturation after radiation.

lysosomal acidity was measured using pH-sensitive probes—acridine orange (AO) and LysoTracker Red (LTR)—with ammonium chloride (AC) as a control. The combination treatment did not alter the fluorescence intensity of these probes, suggesting that lysosomal acidity remained stable (Fig. 4C-D). Lastly, the lysosomal protein degradation capacity was evaluated through a dye-quenched bovine serum albumin (DQ-BSA) assay. Both WA and the combination treatments significantly reduced DQ-BSA-associated red fluorescence, indicating an impaired lysosomal degradation of protein cargo (Fig. 4E-F). Collectively, these findings suggest that WA impairs autophagosome-lysosome fusion and lysosomal degradation.

Combination of WA and Radiation Alters Cellular Bioenergetics.

To assess the effects on cellular bioenergetics, SGC-7901 cells were treated with WA, IR, and their combination, with mitochondrial function analyzed using the Seahorse XF Cell Mito Stress Test Kit. Treatment with either IR, WA, or their combination increased the basal oxygen consumption rate (OCR) (Fig. 5A), likely as

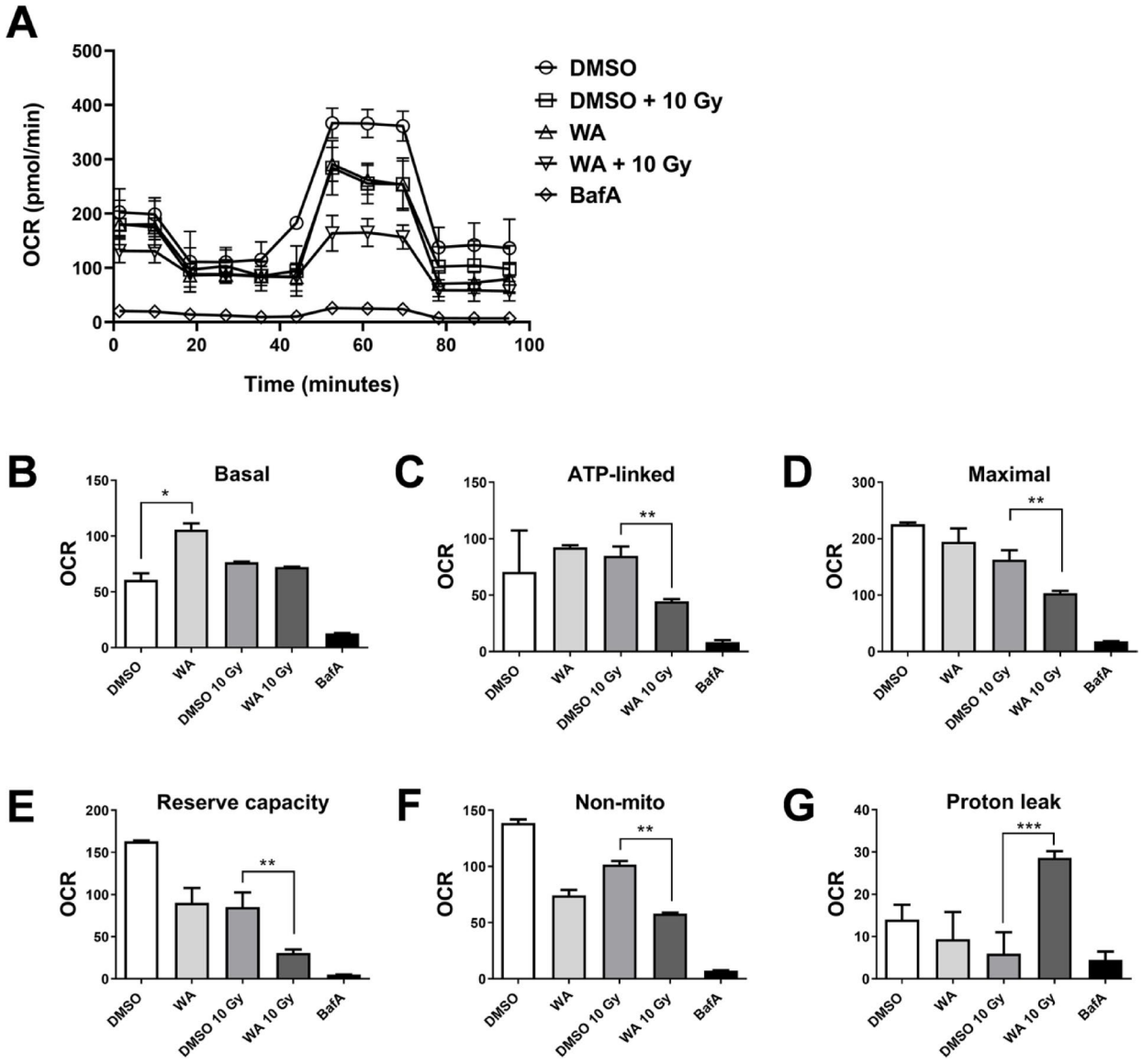

Fig. 5. Effects of the combination of radiation and WA on GC cell bioenergetics. (**A**) The oxygen consumption rate (OCR) in SGC-7901 cells exposed to WA (20 μM) or bafilomycin (10 nM) and 10 Gy radiation was determined by a mitochondrial stress test. (**B**-**G**) ATP-linked, maximal, reserve capacity, proton leakage, and nonmitochondrial OCR were calculated from (**A**) as described in the Methods. The data are the mean and SD of three independent repeats. All the results were shown as mean ± SD ($n = 3$). $^{*}P < 0.05$, $^{**}P < 0.01$ and $^{***}P < 0.001$.

a regulatory response to stress. Notably, the combined treatment resulted in a significantly lower OCR compared to either IR or WA alone. Furthermore, compared to IR treatment, the combined treatment with WA and IR led to significantly decreased ATP-linked OCR, maximal respiration, reserve capacity, and nonmitochondrial OCR values, along with a marked increase in proton leakage (Fig. 5B-G). These findings suggest that WA-related damage to mitochondrial integrity and quality following radiation exposure contributes to cell death.

Combination of withaferin A and radiation inhibits tumor growth and enhances radiosensitivity in vivo

To examine the in vivo impact of Withaferin A (WA) and radiation (IR) on tumor growth, SGC-7901 gastric cancer xenografts were established by subcutaneously injecting tumor cells into the flanks of nu/nu mice. Once tumors reached approximately 100 mm^3, mice were divided into four treatment groups: (1) control (PBS), (2) WA (2 mg/kg), (3) IR (10 Gy), and (4) a combination of IR and WA. Treatments were administered every other day for 21 days, and tumor volume was monitored bi-daily. While tumor volumes in the control and WA-only groups were comparable, the combination of IR and WA significantly inhibited tumor growth, as indicated by reduced tumor size and weight at day 21 (Fig. 6A-C). Immunohistochemical staining revealed reduced Ki67 and

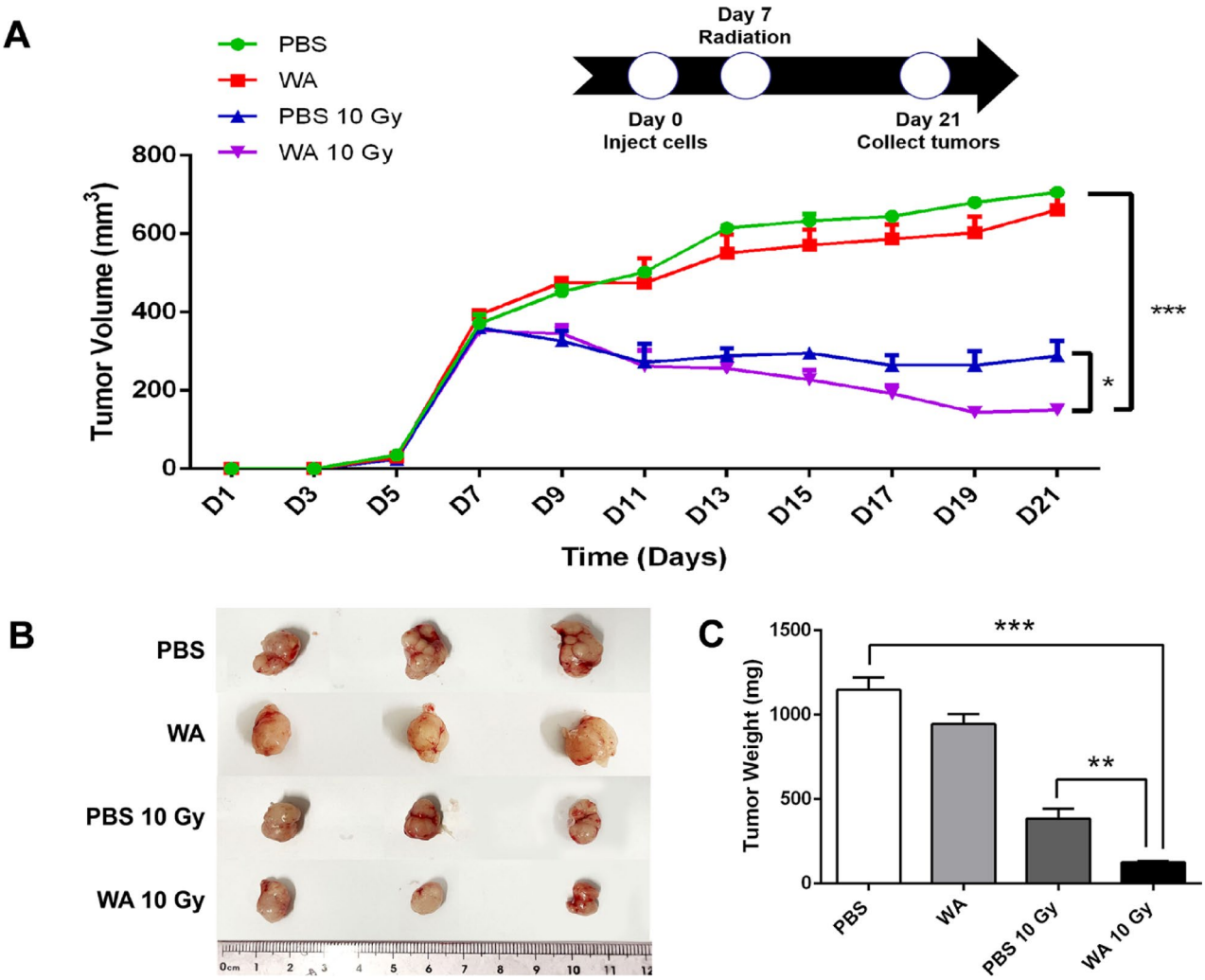

Fig. 6. The combination of WA and radiation increases the radiosensitivity of gastric cancer cells in vivo. Xenografts were established in nude mice to examine whether WA can increase the radiosensitivity of gastric cancer in vivo. Each group of mice was composed of three male nude mice. Tumour sizes were measured at 2-day intervals. (**A**) There was no difference between the PBS group and the WA group. However, gastric cancer cell growth was effectively suppressed in the combined treatment group compared with the 10 Gy X-ray irradiation group. (**B**) Tumour xenografts from each group. (**C**) The weights of tumours collected immediately after sacrifice on day 21. Three representative tumor samples were shown per group although five mice were used in each group. All the results were shown as mean ± SD ($n = 5$). $^{*}P < 0.05$, $^{**}P < 0.01$ and $^{***}P < 0.001$.

CD31 expression in the combination group, indicating suppressed proliferation and angiogenesis (Fig. 7). These findings suggest that combining WA with radiation results in a synergistic inhibition of tumor growth.

Discussion

Radiosensitizers improve the efficacy of radiotherapy by enhancing the cytotoxic effect of radiation[22]. Thus far, studies on radiosensitizers have focused mainly on targeting DNA repair, the cell cycle, telomeres, growth signalling pathways, angiogenesis, cellular bioenergetics, inflammation, hypoxia, and invasion and metastasis proteins; overcoming resistance to cell death; and activating host immunity[23,24]. Recently, the therapeutic potential of herbal ingredients has attracted much attention because of the low toxicity and high efficacy of these substances[25,26]. Herbal ingredients can reduce the side effects of radiotherapy in patients with cancer and improve patients' clinical symptoms by promoting apoptosis and autophagy[27]inhibiting the proliferation and migration of tumour cells[28]blocking cell cycle progression, and inhibiting the production of vascular endothelial growth factor. Herbal ingredients may be beneficial in combination with radiotherapy and may be useful as effective radiosensitizers[25]. This study revealed that Withaferin A (WA), in combination with radiation (IR), significantly enhances the radiosensitivity of gastric cancer cells by modulating apoptosis, autophagy, and mitochondrial function. The combined WA and IR treatment inhibited tumor growth both in vivo and in vitro, highlighting a synergistic effect that holds promise for enhancing therapeutic outcomes in gastric cancer treatment.

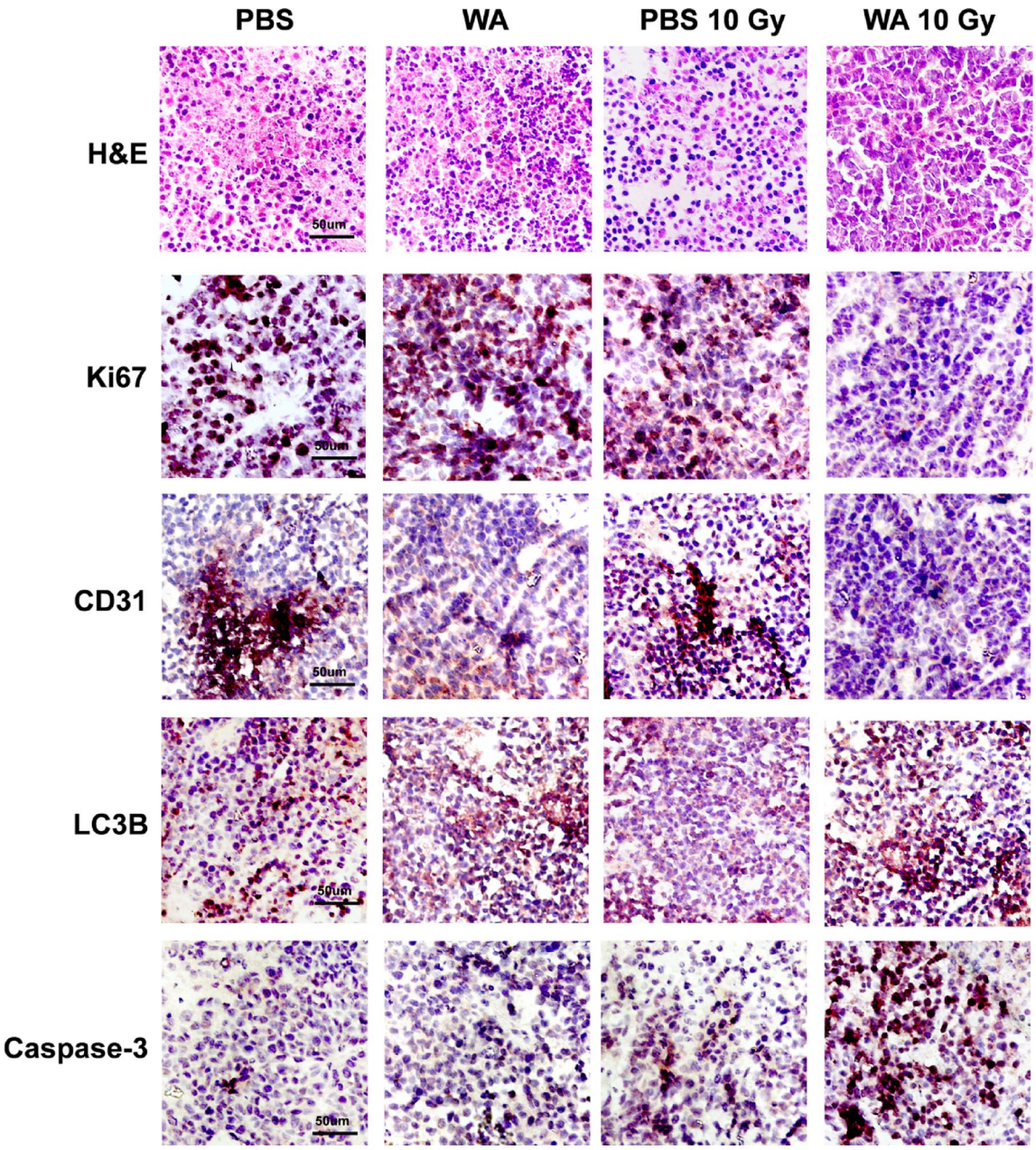

Fig. 7. Immunohistochemistry compilation of tumour tissues. Tumour tissues were developed with DAB (brown) and counterstained with haematoxylin to stain nuclei (blue). Arrows show antibody positive parts. Negative control samples consisted of tissues stained without primary antibody.

One of the primary findings in this study was the potentiation of apoptotic pathways in response to combined WA and radiation treatment. Gastric cancer cells treated with both WA and IR exhibited increased levels of cleaved caspase-3 and PARP, markers of late-stage apoptosis, suggesting a mechanism through which WA amplifies the effects of radiation by promoting cancer cell death. Previous research has shown that WA induces apoptosis in various cancer types through multiple signaling pathways, including BCL2/Bax alteration[29]ERK/Nrf-2/HO-1 activation[8]PI3K/Akt initiation[4]and the phosphorylation and nuclear translocation of Smad2/3 and NF-κB[4]. In this study, the enhanced apoptotic response in gastric cancer cells indicates that WA could overcome cellular mechanisms that typically resist radiation-induced apoptosis, rendering cancer cells more susceptible to radiation therapy.

The study also demonstrated that WA modulates autophagy, a cellular process often hijacked by cancer cells to adapt to therapeutic stress. In the context of radiotherapy, activation of autophagy plays an important role in promoting cancer cell survival in the tumour microenvironment in vivo and contributes to resistance to radiation and DNA damage, thereby sustaining tumour cell survival under stress[30–32]. While autophagy can be protective by enabling cancer cells to cope with metabolic stress, it can also contribute to therapy resistance[33,34]. The present findings suggest that WA disrupts autophagic flux in gastric cancer cells when combined with radiation, as

evidenced by the accumulation of the autophagic substrate SQSTM1/p62 and impaired lysosomal degradation. This blockage may interfere with the ability of cancer cells to recycle damaged cellular components and maintain cellular homeostasis under stress, thereby sensitizing them to radiation-induced damage. Furthermore, autophagy modulation by WA appears to be time-dependent, with early activation of autophagy followed by a block in flux, suggesting that WA may initially activate autophagy as a stress response but subsequently inhibit it to prevent cancer cell adaptation and survival. Similar to our results obtained with WA in GC cells, WA has been shown to induce incomplete autophagy in breast cancer cells[35]indicating the broad-spectrum ability of WA to induce incomplete autophagy.

Interestingly, WA did not significantly alter lysosomal membrane integrity or acidity, but it did inhibit lysosomal degradation capacity, as demonstrated in the DQ-BSA assay. This result suggests that WA specifically disrupts lysosomal function related to autophagic cargo degradation without affecting overall lysosomal stability. The stability of lysosomal membranes alongside reduced degradation capacity implies that WA impairs autophagosome-lysosome fusion or the enzymatic function within lysosomes rather than causing general lysosomal damage. This selective inhibition of lysosomal degradation may serve as an effective strategy to sensitize cancer cells to radiation by specifically targeting the autophagic pathway without affecting other lysosomal functions critical for normal cell maintenance.

Mitochondrial dysfunction emerged as a key factor in the enhanced radiosensitivity observed with the WA and IR combination. The disruption of mitochondrial function is critical for inducing apoptosis, as mitochondrial damage leads to the release of pro-apoptotic factors and triggers a cascade of events that culminates in cell death[36,37]. Additionally, WA's impact on mitochondrial function may amplify the effects of radiation, which also induces oxidative damage in cancer cells. By targeting mitochondrial bioenergetics, WA may sensitize gastric cancer cells to radiation by exacerbating metabolic stress and impairing energy production, ultimately contributing to the observed reduction in cell viability and tumor growth.

In conclusion, the combination of WA and radiation offers a multifaceted approach to gastric cancer therapy, targeting apoptosis, autophagy, and mitochondrial function to enhance radiosensitivity. These results suggest that WA could serve as an effective adjuvant to radiation therapy in gastric cancer, warranting further investigation in clinical settings to validate these findings.

Conclusion

In conclusion, this study demonstrates that Withaferin A (WA) combined with radiation (IR) enhances the radiosensitivity of gastric cancer cells by promoting apoptosis, disrupting autophagic flux, and impairing mitochondrial function. The combined treatment synergistically inhibited tumor growth both in vivo and in vitro, as evidenced by increased apoptotic markers, blocked autophagic degradation, and compromised mitochondrial bioenergetics. These results suggest that WA is a promising adjuvant for radiotherapy, providing a multifaceted strategy to improve therapeutic outcomes in gastric cancer and supporting further investigation in clinical settings.

Data availability

The datasets used and/or analyzed during the current study available from the corresponding author on reasonable request.

Received: 29 November 2024; Accepted: 30 May 2025
Published online: 04 June 2025

References

1. Alsina, M., Arrazubi, V., Diez, M. & Tabernero, J. Current developments in gastric cancer: From molecular profiling to treatment strategy. *Nat. Rev. Gastroenterol. Hepatol.* **20**, 155–170 (2023).
2. Guan, W. L., He, Y. & Xu, R. H. Gastric cancer treatment: Recent progress and future perspectives. *J. Hematol. Oncol.* **16**, 57 (2023).
3. Trautmann, D., Suazo, F., Torres, K. & Simón, L. Antitumor effects of resveratrol opposing mechanisms of helicobacter pylori in gastric cancer. *Nutrients* **16**, 2141 (2024).
4. Kumar, S. et al. Withaferin A: A pleiotropic anticancer agent from the Indian medicinal plant Withania somnifera (L.) Dunal. *Pharmaceuticals* **16**, 160 (2023).
5. Hahm, E. R., Kim, S. H. & Singh, S. V. Withaferin A inhibits breast cancer-induced osteoclast differentiation. *Mol. Carcinog.* **62**, 1051–1061 (2023).
6. Pal, D. et al. Withaferin A: The potent anti-cancer agent from Ashwagandha. *Minerva Biotechnol. Biomol. Res.* **36** (2024).
7. Abeesh, P. & Guruvayoorappan, C. The therapeutic effects of Withaferin A against cancer: Overview and updates. *Curr. Mol. Med.* **24**, 404–418 (2024).
8. Checker, R. et al. Withaferin A, a steroidal lactone, selectively protects normal lymphocytes against ionizing radiation induced apoptosis and genotoxicity via activation of ERK/Nrf-2/HO-1 axis. *Toxicol. Appl. Pharmcol.* **461**, 116389 (2023).
9. Abeesh, P., Guruvayoorappan, C., Withaferin, A-E. & PEGylated Nanoliposomes induce apoptosis in B16F10 melanoma cells by regulating Bcl2 and Bcl Xl genes and mitigates murine solid tumor development. *J. Environ. Pathol. Toxicol. Oncol.* **43** (2024).
10. Zhu, H. et al. Withaferin a modulation of microglia autophagy mitigates neuroinflammation and enhances cognitive function in POCD. (2023).
11. Chen, X. et al. Withaferin A, a natural thioredoxin reductase 1 (TrxR1) inhibitor, synergistically enhances the antitumor efficacy of Sorafenib through ROS-mediated ER stress and DNA damage in hepatocellular carcinoma cells. *Phytomedicine* **128**, 155317 (2024).
12. Kumar, P. et al. Revisiting the multifaceted therapeutic potential of Withaferin A (WA), a novel steroidal lactone, W-ferinAmax ashwagandha, from Withania Somnifera (L) Dunal. *J. Am. Nutr. Assoc.* **43**, 115–130 (2024).
13. Zhou, X. et al. Withaferin A inhibits liver cancer tumorigenesis by suppressing aerobic glycolysis through the p53/IDH1/HIF-1α signaling Axis. *Curr. Cancer Drug. Targets.* **24**, 534–545 (2024).
14. Zhang, J. et al. Autophagy regulators in cancer. *Int. J. Mol. Sci.* **24**, 10944 (2023).

15. Anitha, K. et al. *In role of autophagy and reactive oxygen species in cancer treatment: principles and current strategies* 73–93 (Springer, 2024).
16. Zhang, P. et al. The role of autophagy in regulating metabolism in the tumor microenvironment. *Genes Dis.* **10**, 447–456 (2023).
17. Hassan, A. M. I. A., Zhao, Y., Chen, X. & He, C. Blockage of autophagy for cancer therapy: A comprehensive review. *Int. J. Mol. Sci.* **25**, 7459 (2024).
18. Lee, M. J., Park, J. S., Jo, S. B. & Joe, Y. A. Enhancing anti-cancer therapy with selective autophagy inhibitors by targeting protective autophagy. *Biomol. Ther.* **31**, 1 (2023).
19. Chen, F. et al. The role of mitochondria in tumor metastasis and advances in mitochondria-targeted cancer therapy. *Cancer Metastasis Rev.*, 1–25 (2024).
20. Yang, Y. et al. The mechanisms of action of mitochondrial targeting agents in cancer: Inhibiting oxidative phosphorylation and inducing apoptosis. *Front. Pharmacol.* **14**, 1243613 (2023).
21. Musicco, C., Signorile, A., Pesce, V., Loguercio Polosa, P. & Cormio, A. Mitochondria deregulations in cancer offer several potential targets of therapeutic interventions. *Int. J. Mol. Sci.* **24**, 10420 (2023).
22. Wang, H., Mu, X., He, H. & Zhang, X. D. Cancer radiosensitizers. *Trends Pharmacol. Sci.* **39**, 24–48 (2018).
23. Barazzuol, L. et al. Radiosensitization of glioblastoma cells using a histone deacetylase inhibitor (SAHA) comparing carbon ions with X-rays. *Int. J. Radiat. Biol.* **91**, 90–98 (2015).
24. Rae, C. & Mairs, R. J. Evaluation of the radiosensitizing potency of chemotherapeutic agents in prostate cancer cells. *Int. J. Radiat. Biol.* **93**, 194–203 (2017).
25. Ge, L. et al. Network meta-analysis of Chinese herb injections combined with FOLFOX chemotherapy in the treatment of advanced colorectal cancer. *J. Clin. Pharm. Ther.* **41**, 383–391 (2016).
26. Kuruba, V. & Gollapalli, P. Natural radioprotectors and their impact on cancer drug discovery. *Radiat. Oncol. J.* **36**, 265 (2018).
27. Gao, P., Hao, F., Dong, X. & Qiu, Y. The role of autophagy and Beclin-1 in radiotherapy-induced apoptosis in thyroid carcinoma cells. *Int. J. Clin. Exp. Pathol.* **12**, 885 (2019).
28. Jiang, M. et al. Dying tumor cell-derived Exosomal miR-194-5p potentiates survival and repopulation of tumor repopulating cells upon radiotherapy in pancreatic cancer. *Mol. Cancer.* **19**, 1–15 (2020).
29. Maarouf, R. E., Azab, K. S., Fatih, E., Helal, N. M., Rashed, L. & H. & Withania somnifera alter BCL2/Bax signaling and trigger apoptosis of MCF-7 and MDA-MB231 breast cancer cells exposed to γ-radiation. *Hum. Exp. Toxicol.* **42**, 09603271231180849 (2023).
30. Li, X., He, S. & Ma, B. Autophagy and autophagy-related proteins in cancer. *Mol. Cancer.* **19**, 1–16 (2020).
31. Xia, D. et al. Nrf2 promotes esophageal squamous cell carcinoma (ESCC) resistance to radiotherapy through the CaMKIIα-associated activation of autophagy. *Cell. Biosci.* **10**, 1–12 (2020).
32. Gao, L., Zheng, H., Cai, Q. & Wei, L. in *Autophagy: Biology and Diseases* 375–387 (Springer, 2020).
33. Bashiri, H. & Tabatabaeian, H. Autophagy: A potential therapeutic target to tackle drug resistance in multiple myeloma. *Int. J. Mol. Sci.* **24**, 6019 (2023).
34. Qin, Y. et al. Autophagy and cancer drug resistance in dialogue: Pre-clinical and clinical evidence. *Cancer Lett.* 216307 (2023).
35. Muniraj, N. et al. Withaferin A inhibits lysosomal activity to block autophagic flux and induces apoptosis via energetic impairment in breast cancer cells. *Carcinogenesis* **40**, 1110–1120 (2019).
36. Nguyen, T. T. et al. Mitochondria-associated programmed cell death as a therapeutic target for age-related disease. *Exp. Mol. Med.* **55**, 1595–1619 (2023).
37. Marzetti, E., Calvani, R., Landi, F., Coelho-Júnior, H. J. & Picca, A. Mitochondrial quality control processes at the crossroads of cell death and survival: Mechanisms and signaling pathways. *Int. J. Mol. Sci.* **25**, 7305 (2024).

Author contributions
Ping Lu and Xuemeng Ji jointly conceived, designed, and conducted the study, as well as drafted this manuscript. Juan Xue reviewed and revised this manuscript.

Funding
This work was supported by Tianjin Key Medical Discipline (Specialty) Construction Project.

Declarations

Competing interests
The authors declare no competing interests.

Ethics statement
All animal experiments were carried out in compliance with the National Institutes of Health guide for the care and use of Laboratory animals (NIH Publications No. 8023, revised 1978) and were approved by the Institutional Animal Care and Use Committee (IACUC) of Tianjin Institute of Radiation Medicine (TIRM-IACUC-2022-0032).

Additional information
Supplementary Information The online version contains supplementary material available at https://doi.org/10.1038/s41598-025-05008-x.

Correspondence and requests for materials should be addressed to P.L. or X.J.